

# Numerical Study of Allowable Current Density for Electromigration Damage of Multilevel Interconnection in Integrated Circuit

**Kazuhiko Sasagawa<sup>1,\*</sup>, Kazuhiro Fujisaki<sup>1</sup>, Takahiro Yanagi<sup>1</sup>**

<sup>1</sup> Department of Intelligent Machines and System Engineering, Hirosaki University, Hirosaki, 036-8561, Japan

\* Corresponding author: sasagawa@cc.hirosaki-u.ac.jp

---

**Abstract** The high current density occurring in integrated circuits induces electromigration (EM) of the metal lines used for electric wirings. A void is formed by EM in the line material and the growth of void leads to the line failure. Recently, multilevel interconnection is widely used in electronics devices and MEMS by connecting upper and lower metal lines through vias. The reservoir structure is often constructed in the multilevel interconnection. It is known that there is threshold current density of EM damage in multilevel interconnection with vias. It is important to evaluate the threshold for determination of allowable electric current in the interconnection. In this study, a numerical simulation technique for analyzing the atomic density distribution generated by EM in the line is applied to evaluate the EM risks of metal line in several kinds of the multilevel structures. The thresholds of current density leading to EM change were calculated through the simulations. We confirmed that the atomic density distribution in the line was essential to increase the threshold and to prevent EM damage in the line. And we also showed the simulation technique was useful in the design of safety structure of electric wirings in integrated circuits.

**Keywords** Integrated Circuit, Reliability, Electromigration, Multilevel Interconnection, Allowable Current Density

---

## 1. Introduction

The high current density occurring in integrated circuits induces electromigration (EM) of the metal lines used for electric wirings. EM is a phenomenon that metallic atoms are transported by electron wind and that void, due to depletion of metallic atoms, is formed in the metal line. As the voids are growing the current density in the metal line increases and then the excessive Joule heating leads to metal line failure. Recently, multilevel interconnection is widely used in electronic devices and MEMS by connecting upper and lower metal lines through vias. The structure of interconnect tree and reservoir structure are constructed in the multilevel interconnection. Reservoir structures have an overhang from via connection, and it is usually located at vias on both anode and cathode sides as shown in Fig. 1. Reservoir structure gives delay of EM failure in multilevel interconnection by increasing margin of critical void length. The effect is caused by metallic atoms supplied from the overhanging parts as atom's reservoir to the metal line. The transportation of atoms is induced by tensile stress at the connection part on cathode side via as a result of EM. It is known that there is threshold current density  $j_{th}$  of EM damage in multilevel interconnection with vias. It is important to evaluate the threshold for determination of allowable electric current in the interconnection. Some research groups have developed evaluation method of  $j_{th}$  [1]. The threshold current density is also evaluated by numerical simulation. The building-up process of atomic density distribution in the line is simulated. And the simulation is based on a governing parameter for EM damage in polycrystalline line  $AFD^*_{gen}$  [2]. The parameter is applicable to two-dimensional line shape. Sasagawa et al. have evaluated  $j_{th}$  of several kinds of interconnect tree structure [3]. In this study, a numerical simulation technique for analyzing the atomic density distribution generated by EM in the line is applied to evaluate the EM risks of metal line in several kinds of the reservoir structures. The threshold  $j_{th}$  of several kinds of straight via-connected line with reservoir are evaluated by the numerical simulation. From the evaluation results, reservoir effects on the threshold current density are discussed.

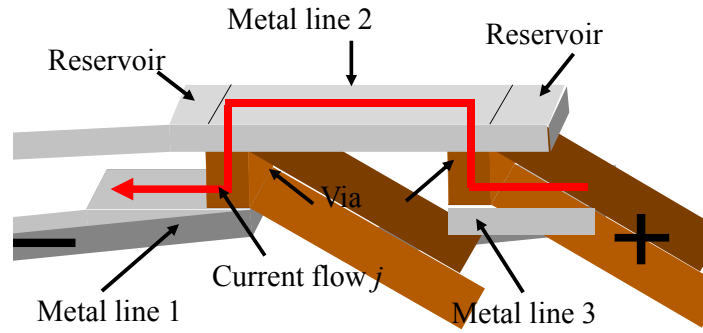


Figure 1. Multilayer interconnection with reservoir structure

## 2. Simulation method

The governing parameter for EM damage is used for constructing the numerical simulation [2]. The parameter is given by formulation of divergence of atomic flux due to EM. The atomic flux vector  $\mathbf{J}$  is represented by Eq. (1).

$$|\mathbf{J}| = \frac{ND_0}{kT} \exp\left\{-\frac{Q_{gb} + \kappa\Omega(N - N_T)/N_0 - \sigma_T\Omega}{kT}\right\} \left( Z^* e \rho j^* - \frac{\kappa\Omega}{N_0} \frac{\partial N}{\partial l} \right) \quad (1)$$

where  $N$  is atomic density,  $D_0$  a prefactor,  $k$  Boltzmann's constant,  $T$  the absolute temperature,  $Q_{gb}$  net activation energy for atomic diffusion,  $\kappa$  the constant relating the change in stress with the change in atomic density under restriction by passivation,  $N_T$  the atomic density under tensile thermal stress  $\sigma_T$ ,  $N_0$  the atomic density at a reference condition,  $\Omega$  the atomic volume,  $Z^*$  the effective valence and  $e$  the electronic charge.  $\rho$  is the temperature-dependent resistivity. Symbols  $j^*$  and  $\partial N/\partial l$  are the components of the current density vector and atomic density gradient in the direction of  $\mathbf{J}$ , respectively. In Eq. (1), the back flow of atoms due to the stress gradient and the effect of the stress generated in the metal line on diffusivity are taken into account.

Grain boundary diffusion is assumed as dominant diffusion mechanism in the simulation, because wide Cu lines covered with passivation layer were supposed. According to literature [4, 5], in wide Cu interconnects, grain boundaries become preferential EM paths rather than lattice and interface diffusions. Sasagawa et al have introduced a grain texture model for calculating atomic flux divergence [6]. So we used the governing parameter for EM damage based on the model even for Cu lines.

Considering atoms going in and out at a unit rectangle, atomic flux divergence in polycrystalline line is formulated as given in Eq. (2).

$$\begin{aligned}
AFD_{gb\theta}^* &= C_{gb}^* N \frac{4}{\sqrt{3}d^2} \frac{1}{T} \exp \left\{ -\frac{Q_{gb} + \kappa\Omega(N - N_T)/N_0 - \sigma_T\Omega}{kT} \right\} \times \\
&\left\langle \sqrt{3}\Delta\varphi \left\{ (j_x \cos \theta + j_y \sin \theta) Z^* e\rho - \frac{\kappa\Omega}{N_0} \left( \frac{\partial N}{\partial x} \cos \theta + \frac{\partial N}{\partial y} \sin \theta \right) \right\} \right. \\
&- \frac{d}{2} \Delta\varphi \left\{ \left( \frac{\partial j_x}{\partial x} - \frac{\partial j_y}{\partial y} \right) Z^* e\rho \cos 2\theta - \frac{\kappa\Omega}{N_0} \left( \frac{\partial^2 N}{\partial x^2} \cos \theta + \frac{\partial^2 N}{\partial y^2} \sin \theta \right) \cos 2\theta \right. \\
&\quad \left. \left. + \left( \frac{\partial j_x}{\partial y} + \frac{\partial j_y}{\partial x} \right) Z^* e\rho \sin 2\theta - 2 \frac{\kappa\Omega}{N_0} \frac{\partial^2 N}{\partial x \partial y} \sin 2\theta \right\} \right. \\
&- \frac{\sqrt{3}}{4} d \frac{\kappa\Omega}{N_0} \left( \frac{\partial^2 N}{\partial x^2} + \frac{\partial^2 N}{\partial y^2} \right) - \frac{\kappa\Omega}{kT} \\
&\quad \times \left[ \frac{\sqrt{3}}{4} d \left\{ Z^* e\rho \left( j_x \frac{\partial N}{\partial x} + j_y \frac{\partial N}{\partial y} \right) - \frac{\kappa\Omega}{N_0} \left( \frac{\partial N}{\partial x} \frac{\partial N}{\partial x} + \frac{\partial N}{\partial y} \frac{\partial N}{\partial y} \right) \right\} \right. \\
&\quad \left. - \frac{d}{2} \Delta\varphi \left\{ Z^* e\rho \left( j_x \frac{\partial N}{\partial y} + j_y \frac{\partial N}{\partial x} \right) - 2 \frac{\kappa\Omega}{N_0} \frac{\partial N}{\partial x} \frac{\partial N}{\partial y} \right\} \sin 2\theta \right] \\
&+ \frac{\sqrt{3}d}{4T} \left\{ \frac{Q_{gb} + \kappa\Omega(N - N_T)/N_0 - \sigma_T\Omega}{kT} - 1 \right\} \\
&\quad \times \left\{ Z^* e\rho \left( j_x \frac{\partial N}{\partial y} + j_y \frac{\partial N}{\partial x} \right) - \frac{\kappa\Omega}{N_0} \left( \frac{\partial N}{\partial x} \frac{\partial N}{\partial x} + \frac{\partial N}{\partial y} \frac{\partial N}{\partial y} \right) \right\} \Bigg\rangle, \tag{2}
\end{aligned}$$

where  $C_{gb}^*$  represents the product  $D_0\delta/k$  denoting the effective width of the grain boundary by  $\delta$ ,  $d$  the average grain size, and  $\Delta\varphi$  a constant related to the relative angle between grain boundaries as shown in Fig. 2. The quantities  $j_x$  and  $j_y$  are components of the current density vector  $\mathbf{j}$  in Cartesian coordinates,  $x$  and  $y$ .  $\theta$  is angle between microstructure unit shown as rectangular in the figure and  $x$  axis.

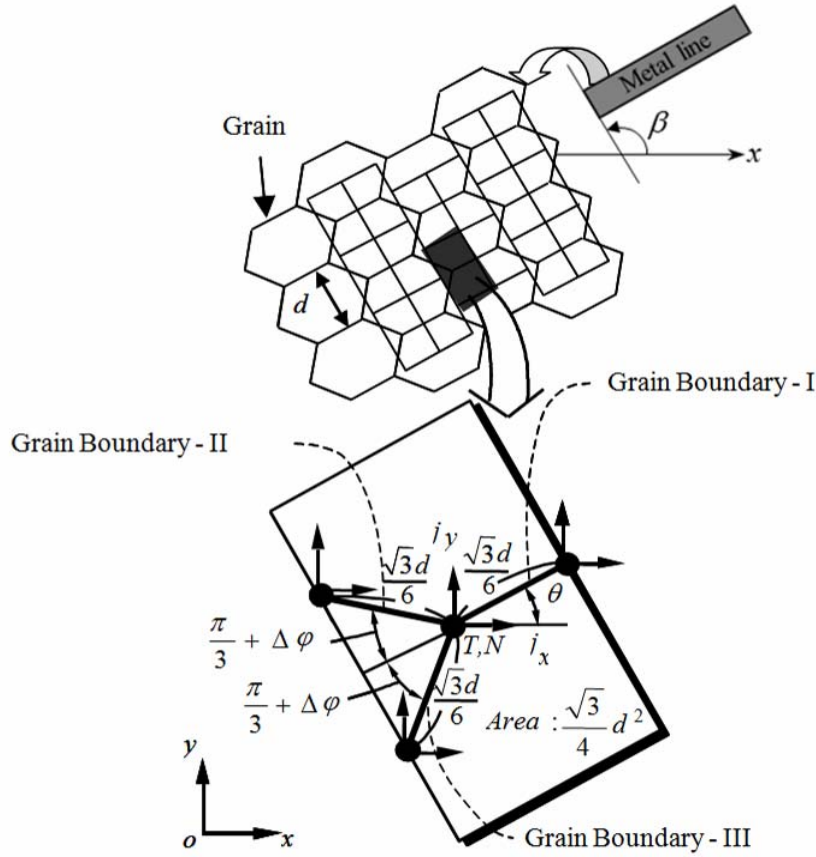


Figure 2. A model of polycrystalline structure

The expectation value of the only positive values of  $AFD^*_{gb\theta}$  is obtained, and it represents the parameter governing EM damage,  $AFD^*_{gen}$ , concerning void formation in a polycrystalline line as

$$AFD^*_{gen} = \frac{1}{4\pi} \int_0^{2\pi} \left( AFD^*_{gb\theta} + \left| AFD^*_{gb\theta} \right| \right) d\theta \quad (3)$$

It means the number of atoms decreasing per unit time and unit volume.

At line ends, boundary condition with respect to atomic flow has to be given for the formulation of the parameter at line ends. Namely, there is no coming-in at cathode end of the line and no going-out at anode one. The boundary condition can be expressed by possible zero flux within the microstructure unit being assigned to each  $\theta$ -range as listed in Table 1 [7].

Table 1. Boundary condition concerning atomic flux

Range-I	Range-II	Range-III
$-2\pi/3 + \Delta\varphi + \beta < \theta \leq -\pi/3 - \Delta\varphi + \beta$	$-\pi/3 - \Delta\varphi + \beta < \theta \leq \beta$	$\beta < \theta \leq \pi/3 + \Delta\varphi + \beta$
$J_{II} = J_{III} = 0$	$J_{II} = 0$	$J_I = J_{II} = 0$
Range-IV	Range-V	Range-VI
$\pi/3 + \Delta\varphi + \beta < \theta \leq 2\pi/3 - \Delta\varphi + \beta$	$2\pi/3 - \Delta\varphi + \beta < \theta \leq \pi + \beta$	$\pi + \beta < \theta \leq 4\pi/3 + \Delta\varphi + \beta$
$J_I = 0$	$J_I = J_{III} = 0$	$J_{III} = 0$

Thus, considering coming and going of atoms within the microstructure unit, the atomic flux divergence at the line end,  $AFD_{\text{gen}}^*|_{\text{end}}$  is expressed by Eq. (4).

$$\begin{aligned}
 AFD_{\text{gen}}^*|_{\text{end}} = & \frac{2}{\sqrt{3}\pi d^2} \frac{C_{gb}^* N}{T} \exp\left(-\frac{Q_{gb} + \kappa\Omega(N - N_T)/N_0 - \sigma_T\Omega}{kT}\right) \left[ 6D_x \sin\beta - 6D_y \cos\beta \right. \\
 & + \frac{\sqrt{3}}{4} \pi d \left\{ -\frac{\kappa\Omega}{N_0} \left( \frac{\partial^2 N}{\partial x^2} + \frac{\partial^2 N}{\partial y^2} \right) - \frac{\kappa\Omega}{kT} \left( D_x \frac{\partial N}{\partial x} + D_y \frac{\partial N}{\partial y} \right) \right. \\
 & \left. \left. + \frac{1}{T} \left( \frac{Q_{gb} + \kappa\Omega(N - N_T)/N_0 - \sigma_T\Omega}{kT} - 1 \right) \left( D_x \frac{\partial T}{\partial x} + D_y \frac{\partial T}{\partial y} \right) \right\} \right] \quad (4)
 \end{aligned}$$

where  $D_x = Z^* e \rho j_x - \kappa\Omega/N_0 (\partial N/\partial x)$ ,  $D_y = Z^* e \rho j_y - \kappa\Omega/N_0 (\partial N/\partial y)$ .  $AFD_{\text{gen}}^*|_{\text{end}}$  expresses the amount of flux divergence at line end and represents the number of atoms decreasing per unit volume and unit time.

Using the governing parameter of EM damage, numerical simulation of atomic density distribution in interconnect is performed under some kinds of input current density,  $j$ , at a certain substrate temperature,  $T_s$ . The line to be evaluated is two-dimensionally divided into elements and building up process of atomic density distribution is simulated by changing the atomic density of each elements based on the parameter. The boundary condition with respect to temperature is given on both line ends and that with respect to current density is given on via position. Atomic flow is insulated around the metal line. The end-parameter  $AFD_{\text{gen}}^*|_{\text{end}}$  is used in elements at cathode and anode ends and on via and  $AFD_{\text{gen}}^*$  is used for elements except both line ends.

The computational procedure is shown in Fig. 3. At first, the distributions of current density and temperature are calculated by two-dimensional FE analysis. The governing parameters are calculated in each element from the analysis results and the film characteristics. Next, the atomic density related to  $\theta$ ,  $N^*$ , is calculated based on the value of the governing parameter. The atomic density in each element  $N$  is calculated by averaging  $N^*$  among all  $\theta$ 's value. By the repetitive calculation, the atomic density distribution in the line grows with time. The iteration is performed until the atomic density reaches a critical atomic density for damage initiation  $N_{\text{min}}^*$  or holds a steady state. If atomic density becomes steady state without reaching  $N_{\text{min}}^*$ , the input current density given in the simulation would be less than  $j_{\text{th}}$ .

### 3. Evaluation

We evaluated four line structures as shown in Fig.4. Sample 1 has no reservoir at both ends of line. Sample 2 has two reservoirs located on both vias. Sample 3 has a reservoir located only on the cathode via. And Sample 4 has a reservoir located only on the anode via. In each sample, the reservoir having shorter length was evaluated. After the simulation with current density smaller than the threshold, a steady state distribution of atomic density should be got without reaching critical atomic density  $N_{\text{min}}^*$ . The smallest value of the atomic density  $N^*$  in all elements at steady state is plotted against supposed current density  $j$ . From an intersection point of the line of the smallest atomic density  $N^*$  and the critical density, the threshold current density is evaluated.

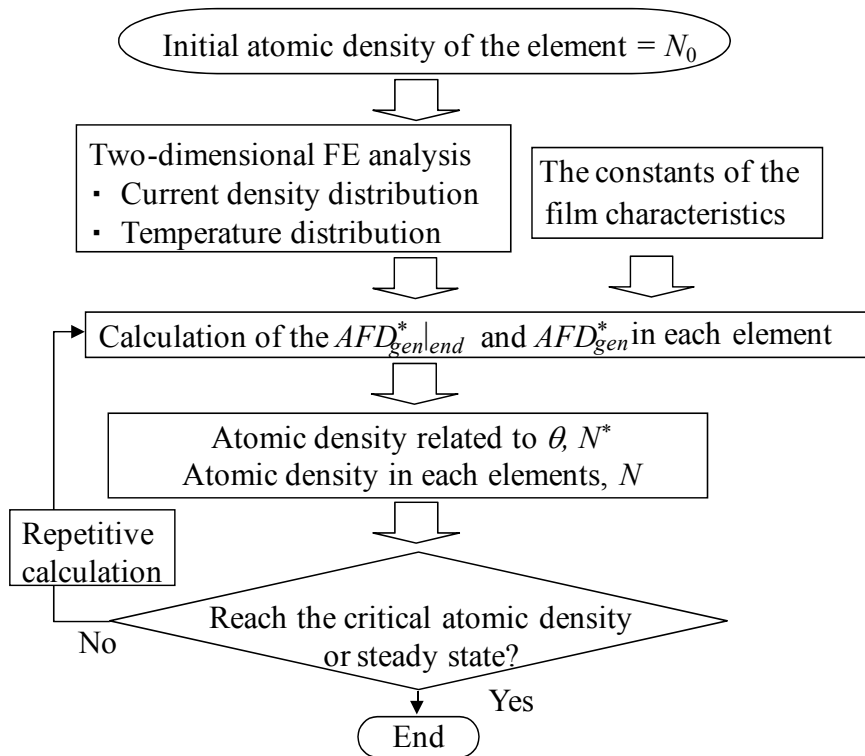


Figure 3. Computational procedure for evaluation of the threshold current density

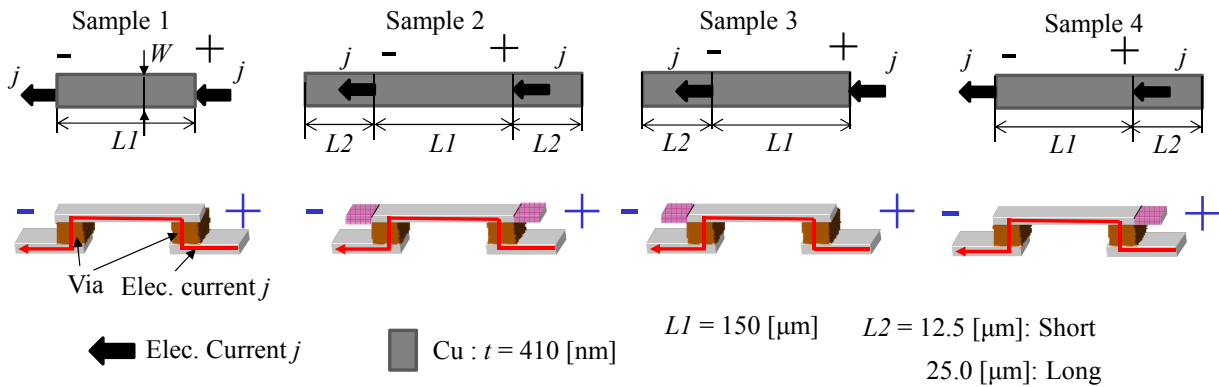


Figure 4. The dimension and structure of the supposed lines

In this simulation, Cu line is assumed having characteristic constants listed in Table 2 [8]-[12]. We supposed three values of input current density, 0.2, 0.4 and 0.6 MA/cm<sup>2</sup>. The operating temperature is assumed 573K for all samples.

Table 2. Characteristic constants used in simulation

Characteristic constants	Value	Reference
$D_0$ [ $\mu\text{m}^2/\text{s}$ ]	3.35	[8]
$Q_{gb}$ [eV]	1.1	[9]
$\Omega$ [ $\mu\text{m}^3$ ]	$3.00 \times 10^{11}$	
$Z^*$	1	[10]
$\rho_0$ [ $\Omega\mu\text{m}$ ]	0.0345 at 573[K]	[11]
$\alpha$ [ $\text{K}^{-1}$ ]	0.0043 at 573[K]	[11]
$\kappa$ [GPa]	42.5	[12]
$N_{min}^*$ [ $\mu\text{m}^{-3}$ ]	$8.40 \times 10^{10}$	[12]
$N_{max}^*$ [ $\mu\text{m}^{-3}$ ]	$8.56 \times 10^{10}$	[12]
$d$ [ $\mu\text{m}$ ]	0.8	

} Cited from results  
for Al interconnect

#### 4. Results and discussion

Figure 5 shows the smallest atomic density calculated in the long type reservoir case. The values of threshold current density  $j_{th}$  were determined in each sample and listed in Table 3. No reservoir and both reservoirs cases (Sample 1 and 2) were almost the same values. The  $j_{th}$  in the cathode reservoir case (Sample 3) showed larger value than those of others. On the other hand, anode reservoir case (Sample 4) showed smaller value than no reservoir case (Sample 1).

According to Eq. (1), if current density is the same, driving force of EM is same. So at steady state, the slope of atomic density corresponds to each other. On the other hand, current density in reservoir is almost zero, and there is not driving force of EM. So at steady state, the slope of atomic density in reservoir becomes almost horizontally. According to conservation law of mass, atomic density distribution in Sample 3 must be shifted upward globally from distribution in Sample 1.

In comparison of length of reservoir, change in  $j_{th}$  from Sample 1 or 2 was enhanced by extension of the reservoir.

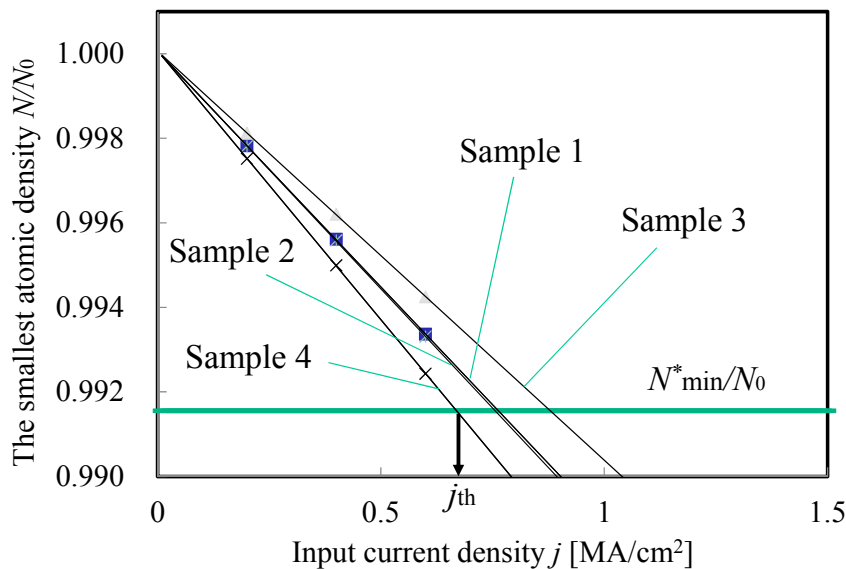


Figure 5. Results of threshold current density in simulation of long type ( $L_2=25 \mu\text{m}$ ) reservoir

Table 3. Threshold values of current density  $j_{th}$  [MA/cm<sup>2</sup>] obtained from simulations

Sample type		1: none	2:+-	3:-	4:+
Reservoir length	Short	0.77	0.76	0.82	0.71
	Long		0.76	0.88	0.67

## 5. Conclusions

The numerical simulation technique was applied to evaluation of reservoir structure and  $AFD_{gen}^*$ -based evaluation of  $j_{th}$  was carried out. We found that if a reservoir is located only on the cathode via, the threshold current density of EM damage is increased. And it was concluded that this phenomenon is caused by the change in atomic density distribution among a metal line.

## Acknowledgments

This work was partly supported by JSPS under Grant-in-Aid for Scientific Research (B) 21360046.

## References

- [1] C. S. Hau-Riege, An introduction to Cu electromigration. *Microelectronics Reliability*, 44 (2004) 195-205.
- [2] H. Abé, K. Sasagawa, M. Saka, Electromigration failure of metal lines. *International Journal of Fracture*, 138 (2006) 219-240.
- [3] K. Sasagawa, T. Abo, Evaluation of threshold current density of electromigration damage in interconnect tree with angled Cu lines. *Proc. of 12th EMAP (2010) Paper ID:230*, 110-116.
- [4] M. H. Lin, K. P. Chang, K. C. Su, T. Wang, Effects of width scaling and layout variation on dual damascene copper interconnect electromigration. *Microelectronics Reliability*, 47 (2007) 2100-2108.
- [5] C. -K. Hu, R. Rosenberg, K. Y. Lee, Electromigration path in Cu thin-film lines. *Applied Physics Letters*, 74 (1999) 2945-2947.
- [6] K. Sasagawa, M. Hasegawa, M. Saka, H. Abé, Governing parameter for electromigration damage in the polycrystalline line with a passivation layer. *Journal of Applied Physics*, 91 (2002) 1882-1890.
- [7] M. Hasegawa, K. Sasagawa, M. Saka, H. Abé, Expression of a governing parameter for electromigration damage on metal line ends. *Proc. of IPACK'03 (CD-ROM), ASME (2003) IPACK2003-35064*.
- [8] Z. S. Choi, R. Ronig, C. V. Thompson, Activation energy and prefactor for surface electromigration and void drift in Cu interconnects. *Journal of Applied Physics*, 102 (2007) 083509.
- [9] C. K. Hu, L. Gignac, R. Rosenberg, Electromigration of Cu/low dielectric constant interconnects. *Microelectronics Reliability*, 46 (2006) 213-231.
- [10] C. L. Gan, C. V. Thompson, K. L. Pey, W. K. Choi, Experimental characterization and modeling of the reliability of three-terminal dual-damascene Cu interconnect trees. *Journal of Applied Physics*, 94 (2003) 1222-1228.
- [11] R. S. Figliola, D. E. Beasley, *Theory and design for mechanical measurements*, Second-ed. John Wiley & Sons, Inc., New York, 1995.
- [12] K. Sasagawa, M. Hasegawa, N. Yoshida, M. Saka, H. Abé, Prediction of electromigration failure in passivated polycrystalline line considering passivation thickness. *Proc. of InterPACK'03 (CD-ROM), ASME (2003) IPACK2003-35065*.